microorganisms

MDPI

Article

The Taxonomic Diversity of Prokaryotic Communities from Permafrost Active Layers of the Chilean Andes

Viktória Faragó [1,2], Andrea K. Borsodi [1,*] and Balázs Nagy [3,4]

[1] Department of Microbiology, ELTE Eötvös Loránd University, H-1117 Budapest, Hungary; viktoriafarago27@gmail.com
[2] Doctoral School of Environmental Sciences, ELTE Eötvös Loránd University, H-1117 Budapest, Hungary
[3] Department of Physical Geography, ELTE Eötvös Loránd University, H-1117 Budapest, Hungary; balazs.nagy@ttk.elte.hu
[4] A Földgömb az Expedíciós Kutatásért Alapítvány, H-1142 Budapest, Hungary
* Correspondence: borsodi.andrea@ttk.elte.hu

Abstract

The study of microorganisms inhabiting extreme environments offers a valuable opportunity to explore their potential ecological roles. This study aimed to reveal and compare the microbial taxonomic diversity of largely unexplored permafrost regions located in different climatic zones (dry and wet) in the Chilean Andes, separated by thousands of kilometers. Permafrost active layer samples were collected from the Ojos del Salado (Atacama Desert) and the Torres del Paine (Patagonia) from different sampling depths. Illumina 16S rRNA gene-based amplicon sequencing revealed that the Andean permafrost active layer provides diverse habitats for distinct microbial communities, with higher taxonomic diversity of Bacteria than Archaea. The wet Patagonian Andes samples showed higher diversity, with a greater abundance of *Chloroflexota* and *Bacteroidota*, while the dry Ojos del Salado samples were dominated by *Actinomycetota*, indicating desiccation stress. Archaea were classified as ammonia-oxidizing members of the *Thermoproteota* phylum. Beta-diversity analyses suggested that differences in environmental conditions (mainly available moisture) contributed more to community structure differentiation than geographical distances. Nevertheless, the effect of sampling depth on microbial diversity was insignificant.

Keywords: permafrost; active layer; extremophiles; microbial diversity; 16S rRNA gene-based amplicon sequencing; microbial ecology

Check for updates

Academic Editors: Panagiota Stathopoulou and Alexander Machado Cardoso

Received: 28 December 2025
Revised: 19 February 2026
Accepted: 4 March 2026
Published: 9 March 2026

Copyright: © 2026 by the authors. Licensee MDPI, Basel, Switzerland. This article is an open access article distributed under the terms and conditions of the Creative Commons Attribution (CC BY) license.

1. Introduction

It is estimated that approximately 11% of Earth's land surface is affected by permafrost on a global scale [1]. Permafrost is defined as ground that remains at or below 0 °C for at least two consecutive years [2]. Permafrost can have the capacity to store about 14.1 Pg (1 Pg = 10^{15} g) of soil organic C (SOC) in the top 3 m, which can be mobilized during permafrost thaw [3]. The upper 1–2 m of the permafrost, known as the active layer, is exposed to freeze-thaw cycles. Due to global warming, the active layer has thickened in numerous regions, leading to increased microbial activity and the release of greenhouse gases, such as methane and carbon dioxide [4]. Given the link between permafrost degradation and the exacerbation of global warming, there has been a surge in research interest in these regions.

Chile has a variety of extreme environments, including the Atacama Desert, which is the driest desert on Earth, as well as ice fields, cold lakes, and glaciers in Patagonia. Ojos

del Salado (6893 m a.s.l.), located in the Dry Andes (27°06′33.84″ S, 68°32′29.63″ W) in the Atacama Desert, is the highest volcano on Earth and the highest mountain without substantial surface ice. Nevertheless, there may still be ground ice within the permafrost. Based on surveys of periglacial landforms and permafrost modeling, ground ice is expected to be above an elevation of 4000–5600 m in the Puna de Atacama [5–7]. The permanent snowline is around 7000 m as a result of severe drought and high irradiation [8]. Most precipitation occurs during the austral summer [9]. The Central Andes, particularly the Puna-Altiplano, has the highest surface solar radiation levels worldwide, with extreme values of approximately 310 W m^{-2} [10]. The area has been designated as a Mars analog research site due to conditions such as low average temperatures, large daily temperature variations, and frozen conditions at night, even during the summer [11].

Patagonia is characterized by a vast network of cold fjords, channels, and oligotrophic cold lakes that extend across southern Chile. The Torres del Paine National Park is located in southern Patagonia, with a total surface close to 181,000 ha, and it is in a transitional forest–steppe zone. The climate is a temperate cold rainy zone without a dry season. Rainfall measurements show significant variation between the eastern and western regions of the park, with annual precipitation ranging from 300 mm in the east to 1500 mm in the west. During the last glacial maximum, the park was entirely covered with ice, resulting in generally young soils [12]. The lithology is derived from volcanic deposits [13].

Microorganisms living in the permafrost have to tolerate sub-zero temperatures, limited water availability, and low-nutrient stress over extended periods of time [14]. Microorganisms capable of thriving in such inhospitable environments are classified as polyextremophiles, indicating their ability to endure multiple extreme conditions at the same time [15]. Despite the harsh environment, relatively high microbial diversity has been observed in permafrost. Certain microorganisms are active even at subzero temperatures. The bacterial diversity present within permafrost is typically higher in comparison to the diversity observed in archaea [16].

In permafrost, the presence of several bacterial phyla, including *Pseudomonadota*, *Chloroflexota*, *Acidobacteriota*, *Actinomycetota*, and *Bacteroidota* have been observed in the Qinghai–Tibet Plateau [17,18], Arctic permafrost [19], and the continuous permafrost region of northeastern China [20]. Previous research has revealed the presence of archaeal sequences, belonging to the *Euryarchaeota*, *Crenarchaeota*, and *Thaumarchaeota* [16]. Additionally, it is common to identify unclassified and novel taxa from extreme environments. The bacterial community of a seasonal high-altitude thaw pond at Ojos del Salado showed moisture-dependent shifts in the relative abundance of *Cyanobacteria* and *Actinomycetota*. The predominant taxa within the community included *Pseudomonadota*, *Bacteroidota*, *Acidobacteriota*, and *Verrucomicrobiota*, with multiple identified orders known for their ability to degrade a broad spectrum of organic compounds [21].

The aim of this study was to gain insight into the microbial taxonomic diversity of the hitherto almost undisturbed and unknown permafrost regions located in different climatic zones of the Andes in Chile. In addition to revealing and comparing the diversity of Bacteria, our research has also focused on uncovering the diversity of previously unknown communities of Archaea. We hypothesize that, although the samples were collected from the active layer of permafrost at both sampling sites, differences in microbial community composition are expected due to variation in geographic latitude and climatic conditions. We further propose that the depth of sampling influences microbial community structure.

2. Materials and Methods

2.1. Description of the Sampling Sites

One sampling area was located in the Dry Andes in northern Chile, and the other was in the Chilean Patagonia (Figure 1). Two sites within the Dry Andes were selected for the collection of samples: the Atacama Camp and the Tejos Camp on the Ojos del Salado. The Ojos del Salado region has been the focus of a decade-long research, resulting in a thorough and well-documented characterization of the area [11,22–27].

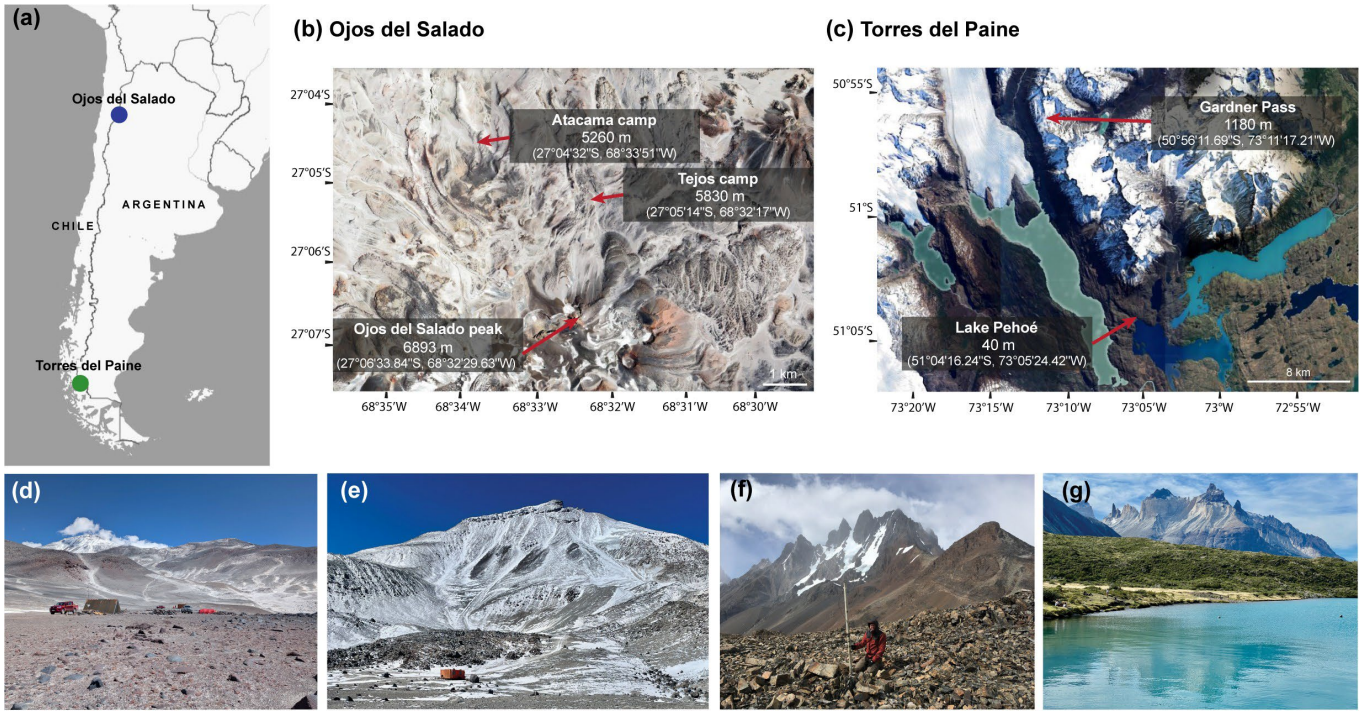


Figure 1. Geographical location of the Ojos del Salado and Torres del Paine sampling sites at (**a**) large scale and (**b**,**c**) local scale. Landscape photograph taken at (**d**) Atacama camp, (**e**) Tejos camp, (**f**) Gardner Pass, and (**g**) Lake Pehoé.

The Atacama camp is located approximately 5.5 km north of the Ojos del Salado massif at an elevation of 5260 m a.s.l, within a flat lava plain. The Tejos site is located approximately 2.5 km north of the Ojos del Salado main volcanic cone, at an elevation of 5830 m a.s.l., in a mountain tundra periglacial environment (Table 1). Surface temperature records at 10 cm depth indicate consistent frost conditions typical of permafrost at the Tejos site, whereas such conditions occur only sporadically at Atacama [25,27]. The active layer is at least >1 m thick at the Atacama, and 70–80 cm at the Tejos camps [26]. Sediments at the Tejos camp are generally coarser than those at Atacama camp. However, the proportion of coarse grains (d > 2 mm) varies with depth, showing the lowest ratios at −35 cm at both the Atacama and the Tejos Camps. At the Atacama site, the bulk density of the regolith was measured 1.3 g/cm^3 at a depth of 10 cm and 1.5 g/cm^3 at depths of 35 and 60 cm. The regolith samples at Tejos Camp show particularly low bulk density, with values of 1.1, 1.3, and 1.0 g/cm^3 at depths of 10, 35, and 60 cm, respectively. At the Atacama site, sediment porosity ranges from 50 to 55% v/v, and water absorption is high only within the upper 10 cm, dropping sharply at greater depths. At the Tejos site, porosity is even higher, ranging between 55 and 67% v/v [24].

The Patagonian samples were collected from the Torres del Paine National Park. One sampling site was located in the mountainous Gardner Pass area, at an elevation of 1180 m a.s.l. (Table 1). These samples originate from the tundra, from periglacial conditions,

and from an extremely windy location. Control samples were collected from the shore of Lake Pehoé at 40 m a.s.l. and 50 m from the lake. Lake Pehoé is a freshwater lake with an irregular shape and a surface area of 22 km^2. The main water input to Lake Pehoé is the Paine River, which flows from Lake Nordenskjöld, and it also receives the outflow from the small Lake Sköttsberg [28]. The low-elevation Torres del Paine site was selected as the control for its undisturbed, postglacial environment, which has geomorphological and climatic characteristics comparable to the mountainous sampling area, except for the presence of permafrost.

Table 1. Environmental and geographical characteristics of the sampling sites.

Location	Ojos del Salado	Ojos del Salado	Torres del Paine	Torres del Paine
Sampling site	Atacama Camp	Tejos Camp	Gardner Pass	Lake Pehoé
Latitude	27°04′32″ S	27°05′14″ S	50°56′11.69″ S	51°04′16.24″ S
Longitude	68°33′51″ W	68°32′17″ W	73°11′17.21″ W	73°05′24.42″ W
Elevation (a.s.l.)	5260 m	5830 m	1180 m	40 m
Sampling time	27 January 2024	29 January 2024	2 March 2024	4 March 2024
Temperature (mean, min, max) [1]	8.8 °C, 3.6 °C, 14.9 °C	3.1 °C, 0.02 °C, 12.8 °C	7.3 °C, 2.9 °C, 12.1 °C	6 °C MAT [2] [29]
Precipitation	150–200 mm/year [30]		1200 mm/year [31]	
Sampling depths (cm)	10, 35, 60	10, 35, 60	10, 35	10, 35
Sample ID	A24	T24	24TK	24TP
Description	Arid, high UV, low bulk density, high porosity		High precipitation, extremely windy	Control samples from the shore of an oligotrophic lake

[1] Temperature values represent a 7-day interval prior to sampling in case of Ojos del Salado and Gardner Pass sampling sites. [2] MAT = mean annual temperature.

2.2. Sampling Process, Soil Chemical Analyses

Ojos del Salado samples were collected at the end of January 2024, and the Torres del Paine samples were taken at the beginning of March 2024. In addition to varying geographical parameters such as latitude and altitude, the samples were collected from multiple depths. Although this study was conducted in permafrost environments, all samples were collected from the active layer, the seasonally thawed layer above the frozen ground. Samples of Ojos del Salado were obtained from depths of 10, 35, and 60 cm, while Torres del Paine samples were collected from 10 and 35 cm depths. Two replicate samples were collected at each site and depth. All samples were collected into 50 mL sterile Falcon tubes (Corning, NY, USA) and kept cool until arriving at the laboratory, where they were stored at 10 °C.

Soil samples were air-dried at room temperature before the concentrations of total carbon, nitrogen, and sulfur were determined using a Vario MAX cube CNS analyzer (Elementar, Langenselbold, Germany).

2.3. Environmental DNA Extraction and 16S rRNA Amplicon Sequencing

The environmental DNAs from the samples were extracted using a DNeasy PowerSoil Pro Kit (QIAGEN, Hilden, Germany). In consideration of the oligotrophic characteristics of the sampling sites, low DNA concentrations were expected. Therefore, 400–500 mg per sample was used, instead of the recommended 250 mg. Due to the limited number of replicates, parallel DNA extractions and PCR amplifications were performed for each sample to enhance reproducibility. The samples were then pooled prior to sequencing.

The PCR was performed using Bacteria-specific (Bakt_341F: 5′-CCTACGGGNGGCWGCAG-3′ and Bakt_805R: 5′-GACTACNVGGGTATCTAATCC-3′) [32] and Archaea-specific (A519F: 5′-CAGCMGCCGCGGTAA-3′ and Arch855R: 5′-TCCCCCGCCAATTCCTTTAA-3′) [33] primers targeting the V3–V4 variable regions of the 16S rRNA gene. The 5′ end of

all primers was elongated with overhang adapters for the Illumina sequencing, provided by SEQme (Dobris, Czech Republic). The adapter sequence for the forward primers was 5′-TCGTCGGCAGCGTCAGATGTGTATAAGAGACAG′ and 5′-GTCTCGTGGGCTCGGAGATGTGTATAAGAGACAG′ for the reverse.

A 20 µL PCR premix was prepared according to the following protocol: 4 µL 5X Phusion HF Buffer, 0.4 µL BSA (20 mg/mL), 0.4 µL 10 mM dNTPs (200 µM each), 0.2 µL 40 µM primers, 0.2 µL Phusion Hot Start II High-Fidelity DNA Polymerase (2 U/µL, Thermo Fisher Scientific, Waltham, MA, USA), 3 or 5 µL DNA template and nuclease free water add to 20 µL. The PCR heat profiles were described by Megyes et al. [34]; the annelation temperature was 55 °C for Bacteria and 60 °C for Archaea. In certain instances, particularly for samples isolated at elevations above 5000 m a.s.l., the number of PCR cycles was increased from 25 to 28. The presence of PCR products was subsequently confirmed through gel electrophoresis using a 1% agarose gel. After pooling the parallels, the concentration of the PCR products was measured using the Qubit assay (Thermo Fisher Scientific, Waltham, MA, USA). Illumina sequencing was carried out by SEQme (Dobris, Czech Republic).

2.4. Data Analysis and Statistics

Sequence reads were analyzed in R version 4.3.0 [35] with the DADA2 package 1.28.0 [36] following the instructions on DADA2′s official website (https://benjjneb.github.io/dada2/tutorial.html accessed on 26 October 2025, DADA2 Pipeline Tutorial version 1.16). Taxonomy was assigned to bacterial and archaeal sequence variants using the Silva database version 138.2 [37].

The data analysis was performed using the phyloseq package version 1.44.0 [38]. The phyloseq object was used to integrate Amplicon Sequence Variant (ASV) abundance tables, taxonomic assignments, and metadata into a unified data frame, thereby enabling consistent downstream analyses such as diversity estimation, relative abundance visualization, ordination, and statistics.

Alpha diversity indices were calculated by subsampling the dataset to the smallest library size for Bacteria (n = 12,646). The archaeal sequencing of three samples resulted in libraries containing fewer than 1000 reads. Therefore, the alpha diversity for Archaea was determined using relative abundances. Shannon and Inverse Simpson indices were calculated using the estimate_richness function of the phyloseq package version 1.44.0. Statistical differences among sampling places were assessed by one-way analysis of variance (ANOVA) followed by Tukey's honest significant difference (HSD) post hoc tests using base R functions. The grouping of letters indicating significant differences was generated with the multcompLetters4 function from the multcompView package version 0.1.10 [39]. The visualization was carried out with the ggplot2 package version 4.0.1 [40].

The relative abundance heatmaps and dendrograms were created with the pheatmap package version 1.0.13 [41]. Stacked bar charts were created with dplyr version 1.1.4 [42] and ggplot2 version 4.0.1. Bacterial phyla that were not detected at ≥1% in at least one sample were grouped into the "Others" category. This threshold for bacterial orders was ≥3%, and for Archaea, no threshold was applied.

Beta diversity was assessed based on Bray–Curtis similarity matrices computed with the vegan package version 2.6.10 [43], then non-metric multidimensional scaling (NMDS) was performed to visualize the differences between the samples. Differences in community composition among sampling sites were tested by permutational multivariate analysis of variance (PERMANOVA) using the adonis2 function from the vegan package version 2.6.10. All PERMANOVA tests were performed with 999 permutations.

Differential abundance analysis at the order level was performed using MaAsLin2 (Microbiome Multivariable Associations with Linear Models) version 1.14.1 in R version 4.3.0 [44], with sampling sites as a fixed effect and Control as the reference site. Abundances were normalized with total sum scale (TSS). For Bacteria, only those orders were retained that appeared in $\geq$1% in at least one sample.

3. Results and Discussion

The relative abundance tables, the number of reads, and ASVs derived from next-generation sequencing are provided in Tables S1–S3. The microbial communities were dominated by bacterial taxa in terms of observed diversity, while archaeal taxa were less diverse. Rarefaction curves were sufficient for both prokaryotic groups, even though Archaea had a very low number of reads in some samples (Figure S1).

Although permafrost environments are generally expected to harbor low archaeal biomass [45–48], the relatively small number of archaeal reads observed in some samples may be influenced by primer bias. In silico evaluations have shown that the commonly used primers (A519F, A855R) incompletely cover certain archaeal phyla. This can lead to the under-representation of specific taxa in amplicon libraries [33,49]. Thus, the low archaeal read counts in our study may reflect a combination of genuinely low abundance of these microorganisms in the studied extreme environments and incomplete amplification due to primer bias.

3.1. Alpha Diversity of Bacteria

Despite the harsh environmental conditions, a high level of bacterial diversity was observed in the active layer (Figure 2). The highest bacterial alpha diversity was observed in samples from Gardner Pass (Shannon: 6.18–6.75, Inverse Simpson: 189.38–597.06). The elevated alpha diversity observed in this region suggests a substantial capacity for diverse microorganisms to colonize this environment. The region represents wet tundra conditions with high precipitation and intense winds, which may enhance microbial dispersal and broaden the range of taxa in the environment. The control samples were expected to have a higher diversity than the other samples, yet this hypothesis was not supported by the data. It is possible that differences in soil texture, moisture, nutrient content, or microhabitat heterogeneity contributed to these results, although no quantitative measurements are available to support this statement. Despite the inhospitable conditions of Ojos del Salado, its microbial composition does not appear reduced, large number of species can be detected. As previously reported, high alpha diversity is present in the upper layer of permafrost-affected areas. Studies have indicated that the Shannon values from the active layer can reach even higher levels [20,50].

ANOVA performed on the Shannon and the Inverse Simpson diversity values revealed differences between the sampling sites, as indicated by letters in Figure 2. A comparison of sampling locations (Torres del Paine or Ojos del Salado) and depths (10, 35, 60 cm) did not reveal clear differences in the diversity indices.

Despite similar alpha diversity indices between wet and dry regions, wet soils showed a higher number of ASVs (Table S3). This finding may suggest that higher moisture conditions are associated with the presence of low-abundance taxa or habitat specialists within a community, which is consistent with the results of Waqas et al. [51], who examined Alaskan permafrost and reported that the bacterial alpha diversity, as measured by the Observed and Chao1 indices, exhibited a significant increase in wet sites compared to dry sites.

3.2. Beta Diversity of Bacteria

In the NMDS analysis (stress level = 0.0458), all four sampling sites form a separate group, and samples from the same region are located close to each other (Figure 3). The

PERMANOVA results indicate that the sampling sites (Control, Gardner Pass, Atacama or Tejos) and regions (Torres del Paine or Ojos del Salado) were associated with differences in bacterial community composition (p-value ≤ 0.001). The sampling site explained a larger proportion of the variance in Bray–Curtis similarities ($R^2 = 0.3819$) compared to the sampling region ($R^2 = 0.1678$). This pattern suggests that site-specific conditions may play a stronger role in shaping bacterial community structure than broader geographical differences. This finding is consistent with a previous study showing that local factors, like soil moisture content, can outweigh climatic or latitudinal gradients in shaping soil microbial communities [52]. The sampling depth was not associated with detectable differences in bacterial community composition (p-value = 0.196).

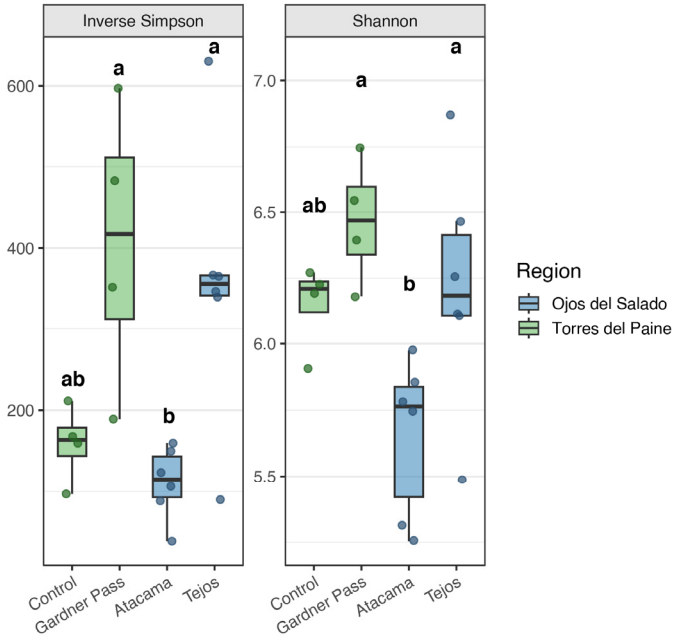


Figure 2. Inverse Simpson and Shannon diversity indices for Bacteria across sampling places. Values were calculated after subsampling to the lowest library size (n = 12,646). Letters above each group indicate statistical differences determined by Tukey's HSD test (groups sharing a letter are not significantly different at $p < 0.05$).

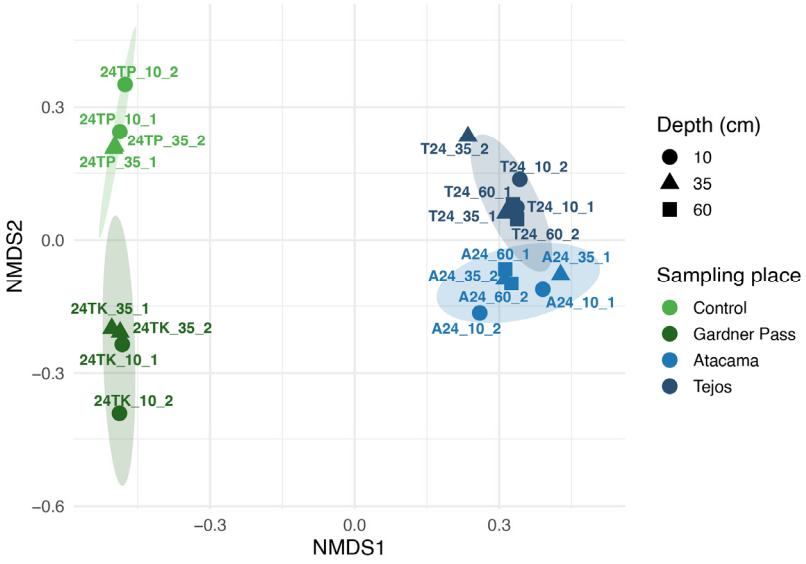


Figure 3. NMDS ordination for Bacteria based on Bray–Curtis distances (stress value = 0.0458).

3.3. Relative Abundance of Bacterial Taxa

All together 42 bacterial phyla were identified, where the most abundant were *Actinomycetota* (37.84%), *Pseudomonadota* (14.84%), *Acidobacteriota* (11.51%), *Chloroflexota* (10.23%), and *Bacteroidota* (10.12%). These phyla are generally reported to be dominant in both high-altitude [18] and tundra soils [50]. Less than 1% of the ASVs were categorized as unclassified phyla (Figure 4a,b).

The Ojos del Salado and Patagonian samples were divided into two groups by the Bray–Curtis dendrograms (Figure 4a,c). The environments of the Atacama and Tejos camps were highly similar, which may provide an explanation for the inaccurate differentiation between the two groups in the dendrograms.

In addition to the presence of permafrost, water availability is a key environmental factor that shapes a microbial community [51]. This study examined samples from the arid regions of the Andes, which were dominated by *Actinomycetota*, a phylum characterized by its high resistance to drought, and have been isolated from the hyperarid-arid margin of the Atacama Desert [53], high-altitude desert soils in the Central Andes exposed to extreme UV radiation [54]. Similarly, in the Barrancas Blancas plain (Puna de Atacama), the driest reference site, located furthest from the temporary lake and under reduced hydrological influence, was dominated by *Actinomycetota* [55], in agreement with our observation that this phylum is associated with drier Andean environments. A comparative study of global active layer microbiomes revealed that the relative abundance of *Actinomycetota* was high in all samples [48]. Members of the *Actinomycetota* can form spores when water decreases in the environment, while others change their cytoplasm structure and cell wall thickness in order to form cyst-like cells, which are more resistant to unfavorable environmental conditions [56,57]. The presence of liquid water and even atmospheric humidity can determine whether cells remain metabolically active or enter dormant states. As water activity declines to approximately 0.88 aw, even highly desiccation-tolerant bacteria may enter a state in which metabolic processes halt, although the cells remain viable [56]. Since DNA is prone to degradation, the long-term survival strategy is more likely that cells remain metabolically active and repair their DNA than to enter dormancy [58]. The large number of *Actinomycetota* in the Ojos del Salado samples may suggest that at the time of sampling, the environments were arid and unfavorable, since the presence of *Actinomycetota* increases with water scarcity [21,51].

From the *Actinomycetota* phylum, the most abundant orders were *Propionibacteriales* and *Solirubrobacterales* in the Ojos del Salado samples (Figure 4c,d). Almost all members of the *Propionibacteriales* order belonged to the *Nocardioidaceae* family (99.8%), and 94.69% of them were classified into the *Nocardioides* genus (Table S1). *Nocardioides* can endure various oligotrophic conditions and are even able to break down several pollutants that are hard to degrade [59], giving them an advantage in low-nutrient environments such as the Ojos del Salado (Table S4). Members of the order *Solirubrobacterales*, particularly the genus *Solirubrobacter,* have been isolated from arid and high UV-exposed environments [60]. In addition to Unclassified genera, *Solirubrobacter* was found in high abundance in all Ojos del Salado samples (Table S1).

Chloroflexota had a high abundance in the Gardner Pass samples, accounting for 22.82–34.27% of the bacterial community in these four samples. The aquatic systems of Torres del Paine are distinguished by their low temperatures, limited nutrients, and low dissolved organic carbon (DOC) concentrations [61]. The studied region receives approximately 1200 mm of precipitation annually [31]. Previous studies found that the abundance of *Chloroflexota* in permafrost is associated with relatively lower nutrient availability and higher moisture content [20], and they revealed that *Chloroflexota* was the dominant phylum in alpine, oligotrophic active layer with mean annual precipitation of 941 mm [45]. In line

with these observations, *Chloroflexota* showed the highest relative abundance in the wet region of the Andes. Similarly, *Bacteroidota* has been reported to have a significant positive correlation with mean annual precipitation [52]. It showed the highest abundance in control samples taken from the shore of an oligotrophic lake in Patagonia.

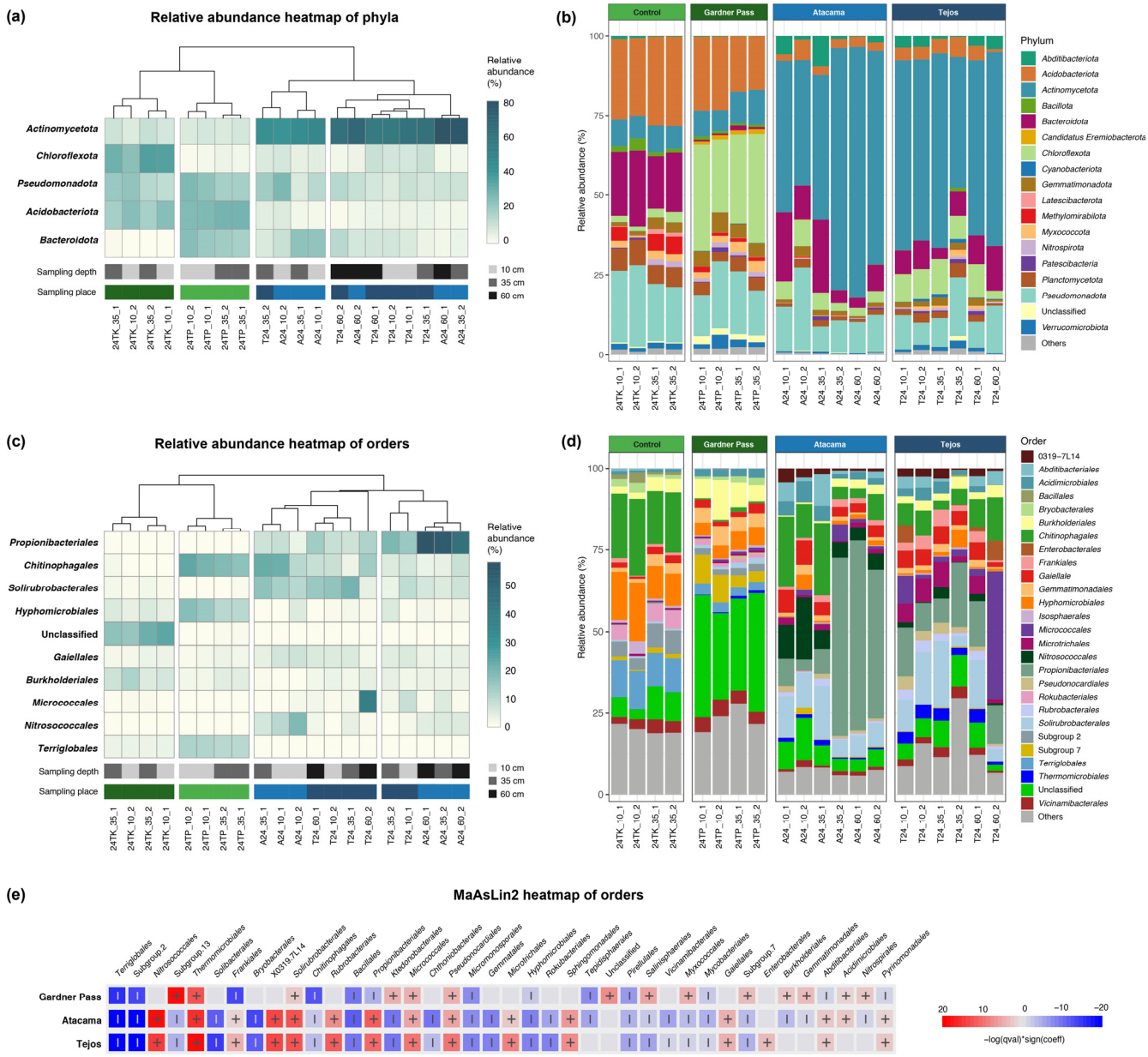


Figure 4. Bacterial community composition at phylum and order taxonomic levels, based on (**a**,**c**) relative abundance heatmaps of most abundant taxa and (**b**,**d**) stacked bar charts. (**e**) Differential abundance analysis of orders across sampling sites using MaAsLin2. The model used Torres del Paine—Control site as a reference. The MaAsLin2 heatmap represents orders that occurred ≥1% of the community in at least one sample.

Our findings indicate that phototrophic taxa did not appear, or their appearance was minimal. Although photosynthetic microorganisms have been isolated from permafrost [62], and high altitude does not exclude the presence of *Cyanobacteria*, as they were reported from 5900 m a.s.l., where liquid water was present [21]. In that prior study, *Cyanobacteria* could not be detected directly on the surface due to high UV radiation, but near the surface or in shaded areas [21]. Samples from the Ojos del Salado analyzed in

this study showed the presence of phyla that indicate aridity, which is unfavorable for *Cyanobacteria* due to their requirement for high water activity (ranges from 1 to 0.6) [63]. The environmental conditions in Torres del Paine do not prevent the emergence of *Cyanobacteria*, but they cannot be detected. It is possible that the presence of these taxa may be suppressed by other taxa, or they might occur closer to the surface than 10 cm. In such extreme environments, suitable niches for *Cyanobacteria* likely require protection from UV radiation and sufficient light. In this study, however, all samples were collected from depths of at least 10 cm, where light penetration was presumably insufficient to support photosynthesis.

Differential abundance analysis using MaAsLin2 identified multiple bacterial orders significantly associated with the sampling sites (Figure 4e). *Terriglobales* and *Solibacterales* were depleted at Atacama and Tejos, while *Nitrosococcales* and *Thermomicrobiales* were enriched at these sites. In accordance with a previous report on hyper-arid Andean environments [64], we identified taxa potentially involved in initial soil formation processes. Members of *Frankiales* were more abundant in the extreme sites of Ojos del Salado, while *Burkholderiales* were primarily associated with the Gardner Pass samples, suggesting a shift in community composition along the environmental gradient.

3.4. Diversity of Archaea

The archaeal pattern of the Ojos del Salado and the Torres del Paine sample from the mountainous region showed differences compared to the control samples, as shown by Tukey's HSD tests in Figure 5.

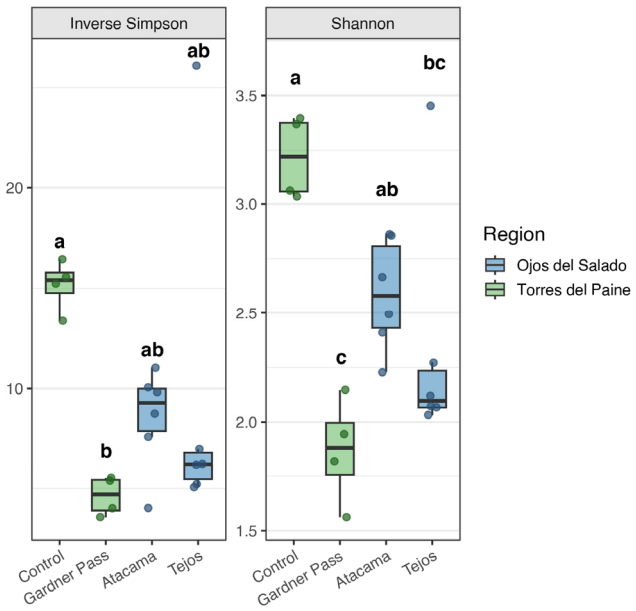


Figure 5. Inverse Simpson and Shannon diversity indices for Archaea across sampling places. Values were normalized by total sum scaling (TSS). Letters above each group indicate statistical differences determined by Tukey's HSD test (groups sharing a letter are not significantly different at $p < 0.05$).

The NMDS analysis (Figure 6) and the PERMANOVA analysis for Archaea showed patterns similar to the bacterial results. The impact of the sampling depth was found to be less considerable than that of the bacterial (p-value = 0.28), while the sampling place (p-value $\leq$ 0.001, R^2 = 0.6388) and sampling region (p-value $\leq$ 0.001, R^2 = 0.3714) were associated with differences in archaeal community composition.

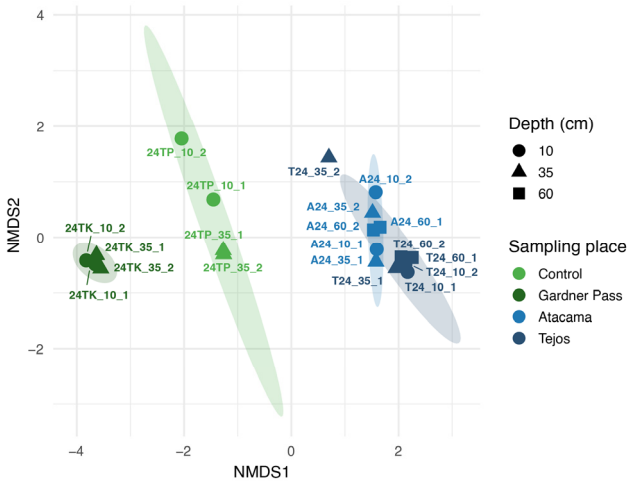


Figure 6. NMDS ordination for Archaea based on Bray–Curtis distances (stress value = 0.0177).

Although the control samples had a higher alpha diversity than the rest of the samples, many ASVs were assigned to unclassified or non-formal archaeal clades such as Marine Group II and Group 1.1c (Figure 7). The differential abundance analysis of archaeal communities (Figure 7e) revealed that members of *Thermoproteota* (previously *Thaumarchaeota*), particularly *Nitrososphaerales*, were enriched at permafrost-related sampling sites, and *Nitrosotaleales* was most abundant at Gardner Pass. These orders are known as ammonia-oxidizing archaea (AOA). They are autotrophic and able to fix their own carbon from inorganic CO_2. Ammonia oxidizers are regarded as specialist microorganisms, as they typically rely on ammonia as the sole source of reducing power. While AOAs are generally adapted to low ammonia concentrations, it is also important to acknowledge that ammonia oxidizers have a wide range of ammonia affinities. Since nitrifiers in the environment are frequently exposed to low and fluctuating substrate concentrations, the affinity for ammonia is likely an important survival factor [65]. Our results indicated that AOA were present in high abundance in permafrost-related environments and were scarce in the control samples.

Although ammonia-oxidizing bacteria (AOB) like *Nitrosococcales* are present in these environments (Figure 4c,d), the dominance of ammonia-oxidizing Archaea suggests that nitrification in these samples is predominantly driven by Archaea. A previous study found that AOB only grew at high ammonia concentrations, while AOA favored low, intermediate, and high ammonia concentrations too [66]. The samples analyzed in this study are characterized as oligotrophic, indicating the presence of AOA rather than AOB (Table S4).

Our research suggests that phototrophic or anaerobic taxa did not appear, or only appeared to a negligible extent, among Bacteria and Archaea. The absence of anaerobic microorganisms is also not evident, 10–15% of anaerobic microorganisms can live in different global permafrost environments [48]. This is likely due to the coarse nature of the analyzed active layer and the strong winds that restricted the presence of anaerobes.

The community composition suggests the presence of chemolithotrophic metabolic strategies, which are advantageous in carbon-limited environments where inorganic electron donors and carbon sources are more consistently available than organic substrates. Waldrop et al. proposed that adaptations to energy acquisition and substrate availability are among the strongest selective pressures shaping permafrost microbial communities [46].

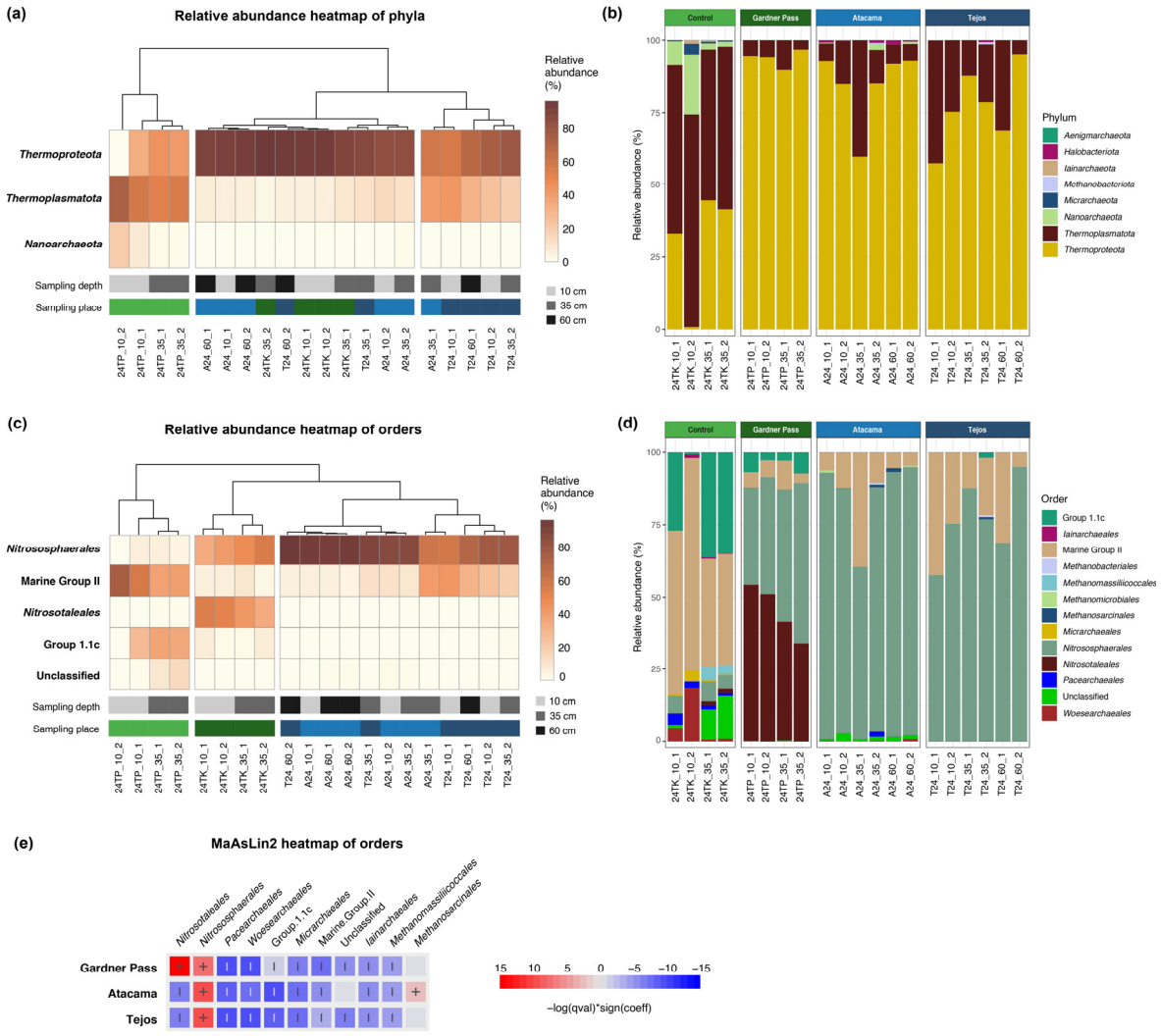


Figure 7. Archaeal community composition at phylum and order taxonomic levels, based on (**a**,**c**) relative abundance heatmaps of most abundant taxa and (**b**,**d**) stacked bar charts. (**e**) Differential abundance analysis of orders across sampling sites using MaAsLin2. The model used Torres del Paine—Control site as a reference.

4. Conclusions

The comparison of prokaryotic taxonomic diversity in the largely unexplored permafrost regions located in different climatic zones (dry and wet) of the Chilean Andes revealed that these environments are inhabited by diverse and distinct microbial communities, characterized by a higher representation of Bacteria rather than Archaea. The structure of bacterial communities may be related to the water activity of the permafrost active layer. The moist Patagonian samples showed higher biodiversity, with larger abundances of *Chloroflexota* and *Bacteroidota*, while the hyper-arid Ojos del Salado samples were dominated by *Actinomycetota*, consistent with extreme drought stress. Archaeal communities were less diverse but exhibited strong functional specialization. The high abundance of ammonia-oxidizing taxa suggests that nitrification is predominantly driven by Archaea in these extreme environments. These findings support our initial hypothesis that geographic and climatic differences shape microbial community composition. However, contrary to our expectations, sampling depth did not have a detectable influence on community structure. The absence of a measurable depth-related effect in this dataset indicates that vertical variations were relatively weak compared to site-specific environmental differences.

Supplementary Materials: The following supporting information can be downloaded at https://www.mdpi.com/article/10.3390/microorganisms14030613/s1. Figure S1: Rarefaction curve for Bacteria and Archaea; Table S1: Relative abundance table for Bacteria; Table S2: Relative abundance table for Archaea; Table S3: Number of reads and ASVs of the samples; Table S4: Soil chemical analyses (C, N, S) of Ojos del Salado samples.

Author Contributions: Conceptualization: A.K.B. and B.N.; Investigation (sample collection): B.N.; Methodology, B.N. and V.F.; Formal analysis: V.F.; Software: V.F.; Data curation: V.F.; Visualization: V.F.; Writing—original draft preparation: V.F.; Writing—review and editing: A.K.B. and B.N.; Supervision: A.K.B. and B.N.; Funding acquisition: B.N. All authors have read and agreed to the published version of the manuscript.

Funding: This research was funded by the National Research, Development and Innovation Office, Hungary (Grants NKFIH OTKA K147424). V. Faragó was supported by the EKÖP-25 University Research Scholarship Program of the Ministry for Culture and Innovation from the Source of the National Research, Development and Innovation fund (EKÖP-25-3-I-ELTE-244).

Institutional Review Board Statement: Not applicable.

Informed Consent Statement: Not applicable.

Data Availability Statement: Raw sequencing data have been deposited in the Sequence Reads Archive under the BioProject accession number: PRJNA1394536.

Acknowledgments: We would like to thank Gergely Krett (ELTE Eötvös Loránd University) for his assistance during laboratory work, and Ágota Horel (HUN-REN ATK, Institute for Soil Sciences) for the soil chemical analysis.

Conflicts of Interest: The authors declare no conflicts of interest.

References

1. Obu, J. How Much of the Earth's Surface Is Underlain by Permafrost? *J. Geophys. Res. Earth Surf.* **2021**, *126*, e2021JF006123. [CrossRef]
2. Everett, K.R. Glossary of Permafrost and Related Ground-Ice Terms. *Arct. Alp. Res.* **1989**, *21*, 55. [CrossRef]
3. Chen, L.; Yang, G.; Bai, Y.; Chang, J.; Qin, S.; Liu, F.; He, M.; Song, Y.; Zhang, F.; Peñuelas, J.; et al. Permafrost Carbon Cycle and Its Dynamics on the Tibetan Plateau. *Sci. China Life Sci.* **2024**, *67*, 1833–1848. [CrossRef] [PubMed]
4. Gilichinsky, D.A.; Wagener, S.; Vishnevetskaya, T.A. Permafrost Microbiology. *Permafr. Periglac. Process.* **1995**, *6*, 281–291. [CrossRef]
5. Trombotto, D. Survey of Cryogenic Processes, Periglacial Forms and Permafrost Conditions in South America. *Rev. Inst. Geológico* **2000**, *21*, 33–55. [CrossRef]
6. Ahumada, A.L. Periglacial Phenomena in the High Mountains of Northwestern Argentina. *S. Afr. J. Sci.* **2002**, *98*, 166–170.
7. Gruber, S. Derivation and Analysis of a High-Resolution Estimate of Global Permafrost Zonation. *Cryosphere* **2012**, *6*, 221–233. [CrossRef]
8. Clapperton, C.M. The Quaternary Glaciation of Chile: A Review. *Rev. Chil. Hist. Nat.* **1994**, *67*, 369–383.
9. Garreaud, R.; Vuille, M.; Clement, A.C. The Climate of the Altiplano: Observed Current Conditions and Mechanisms of Past Changes. *Palaeogeogr. Palaeoclimatol. Palaeoecol.* **2003**, *194*, 5–22. [CrossRef]
10. Albarracín, V.H.; Kurth, D.; Ordoñez, O.F.; Belfiore, C.; Luccini, E.; Salum, G.M.; Piacentini, R.D.; Farías, M.E. High-up: A Remote Reservoir of Microbial Extremophiles in Central Andean Wetlands. *Front. Microbiol.* **2015**, *6*, 1404. [CrossRef]
11. Kereszturi, A.; Aszalos, J.M.; Zs, H.; Igneczi, Á.; Zs, K.; Cs, K.; Sz, L.O.; Szalai, Z.; Zs, N.; Pal, B.; et al. Wind-Snow Interactions at the Ojos Del Salado Region as a Potential Mars Analogue Site in the Altiplano—Atacama Desert Region. *Icarus* **2022**, *378*, 114941. [CrossRef]
12. Mataix-Solera, J.; Arellano, E.C.; Jaña, J.E.; Olivares, L.; Guardiola, J.; Arcenegui, V.; García-Carmona, M.; García-Franco, N.; Valenzuela, P. Soil Vulnerability Indicators to Degradation by Wildfires in Torres Del Paine National Park (Patagonia, Chile). *Span. J. Soil Sci.* **2021**, *11*, 10008. [CrossRef]
13. Cerrillo, R.M.N.; Hayas, A.; García-ferrer, A.; Clemente, R.H.; Duhalde, P.; González, L. Characteristics of Areas Affected by Fire in 2005 at Parque Nacional de Torres Del Paine (Chile) as Assessed from Multispectral Images. *Rev. Chil. Hist. Nat.* **2008**, *81*, 95–110.

14. Goordial, J.; Lamarche-Gagnon, G.; Lay, C.-Y.; Whyte, L. Left Out in the Cold: Life in Cryoenvironments. In *Polyextremophiles: Life Under Multiple Forms of Stress*; Cellular Origin, Life in Extreme Habitats and Astrobiology; Seckbach, J., Oren, A., Stan-Lotter, H., Eds.; Springer: Dordrecht, The Netherlands, 2013; Volume 27, pp. 335–363. [CrossRef]
15. Horikoshi, K.; Bull, A.T. 1.1. Prologue: Definition, Categories, Distribution, Origin and Evolution, Pioneering Studies, and Emerging Fields of Extremophiles. In *Extremophiles Handbook*; Horikoshi, K., Ed.; Springer: Tokyo, Japan, 2011; pp. 3–15. [CrossRef]
16. Jansson, J.K.; Taş, N. The Microbial Ecology of Permafrost. *Nat. Rev. Microbiol.* **2014**, *12*, 414–425. [CrossRef]
17. Chen, S.; Xu, J.; Cao, J.; Bahadur, A.; Wu, M.; Wang, Z.; Chen, J.; Wang, J.; Shi, Y. Depth-Related Microbial Communities and Functional Genes in Alpine Permafrost. *Innov. Life* **2024**, *2*, 100081. [CrossRef]
18. Zhang, W.; Bahadur, A.; Sajjad, W.; Zhang, G.; Nasir, F.; Zhang, B.; Wu, X.; Liu, G.; Chen, T. Bacterial Diversity and Community Composition Distribution in Cold-Desert Habitats of Qinghai—Tibet Plateau, China. *Microorganisms* **2021**, *9*, 262. [CrossRef] [PubMed]
19. Dziurzynski, M.; Gorecki, A.; Pawlowska, J.; Istel, L.; Decewicz, P.; Golec, P.; Styczynski, M.; Poszytek, K.; Rokowska, A.; Gorniak, D.; et al. Revealing the Diversity of Bacteria and Fungi in the Active Layer of Permafrost at Spitsbergen Island (Arctic)—Combining Classical Microbiology and Metabarcoding for Ecological and Bioprospecting Exploration. *Sci. Total Environ.* **2023**, *856*, 159072. [CrossRef] [PubMed]
20. Ren, B.; Hu, Y.; Bu, R. Vertical Distribution Patterns and Drivers of Soil Bacterial Communities across the Continuous Permafrost Region of Northeastern China. *Ecol. Process.* **2022**, *11*, 6. [CrossRef]
21. Faragó, V.; Megyes, M.; Nagy, B.; Hengst, M.; Paquis, P.; Borsodi, A.K. Environmental Characterization and Impact of Climatic Fluctuations on the Diversity of Extremophilic Bacterial Communities of a High-Altitude Seasonal Meltwater Pond on Ojos Del Salado (Dry Andes, Chile). *Geomicrobiol. J.* **2024**, *41*, 1008–1017. [CrossRef]
22. Nagy, B.; László, M.; József, K.; Zsombor, N.; Heiling, Z. Az Ojos Del Salado Monitoring Vizsgálata: Jég- És Vízjelenlét a Föld Legszárazabb Magashegyében BEVEZETÉS. *Földrajzi Közlemények* **2014**, *9*, 452–462.
23. Nagy, B.; Ignéczi, Á.; Kovács, J.; Szalai, Z.; Mari, L. Shallow Ground Temperature Measurements on the Highest Volcano on Earth, Mt. Ojos Del Salado, Arid Andes, Chile. *Permafr. Periglac. Process.* **2018**, *30*, 3–18. [CrossRef]
24. Nagy, B.; Ruiz-Pereira, S.; Kovács, J.; Borsodi, A.; Kern, Z.; Mihajlik, G.; Ignéczi, Á. Exploring the Highest Atacama: Where the Desert Meets the Tundra—Water-Related Processes in the Cold-Dry Environment. In *Advances in Environmental Research*; Daniels, J.A., Ed.; Nova Science Publishers: Hauppauge, NY, USA, 2024; pp. 45–78.
25. Pereira, S.R.; Leray, S.; Marti, E.; Beriain, E.; Suárez, F.; Yáñez, G.; Nagy, B. Assessing Permafrost Structures in Headwater Aquifers: An Example from the Ojos Del Salado Massif, Andes Mountains. *Andean Geol.* **2025**, *52*, 239–253. [CrossRef]
26. Nagy, B.; Kovács, J.; Ignéczi, Á.; Beleznai, S.; Mari, L.; Kereszturi, Á.; Szalai, Z. The Thermal Behavior of Ice-Bearing Ground: The Highest Cold, Dry Desert on Earth as an Analog for Conditions on Mars, at Ojos Del Salado, Puna de Atacama-Altiplano Region. *Astrobiology* **2020**, *20*, 701–722. [CrossRef]
27. Nagy, B.; Ruiz-Pereira, S.; Ignéczi, Á.; Kovács, J.; Ghahraman, K.; Mihajlik, G.; Túri, M.; Kern, Z. Surface Hydrology on the Highest Volcano of the High Dry Andes, the Ojos Del Salado; Interannual Fluctuations and Moisture Sources. *J. Hydrol.* **2025**, *653*, 132741. [CrossRef]
28. TNC. *Plan de Conservación Reserva de la Torres del Paine 2024–2030*; The Nature Conservancy: Santiago, Chile, 2024.
29. Paruelo, J.M.; Beltrán, A.; Jobbágy, E.; Sala, O.E.; Golluscio, R.A. *The Climate of Patagonia: General Patterns and Controls on Biotic Processes*; Asociación Argentina de Ecología: Buenos Aires, Argentina, 1998; Volume 8.
30. Messerli, B.; Grosjean, M.; Vuille, M. Water Availability, Protected Areas, and Natural Resources in the Andean Desert Altiplano. *Mt. Res. Dev.* **1997**, *17*, 229–238. [CrossRef]
31. Fuentes-Aguilera, P.; Rodríguez-López, L.; Bourrel, L.; Frappart, F. Hydroclimatic Variability of the Grey River Basin (Chilean Patagonia): Trends and Relationship with Large-Scale Climatic Phenomena. *Water* **2025**, *17*, 1895. [CrossRef]
32. Herlemann, D.P.R.; Labrenz, M.; Jürgens, K.; Bertilsson, S.; Waniek, J.J.; Andersson, A.F. Transitions in Bacterial Communities along the 2000 Km Salinity Gradient of the Baltic Sea. *ISME J.* **2011**, *5*, 1571–1579. [CrossRef] [PubMed]
33. Klindworth, A.; Pruesse, E.; Schweer, T.; Peplies, J.; Quast, C.; Horn, M.; Glöckner, F.O. Evaluation of General 16S Ribosomal RNA Gene PCR Primers for Classical and Next-Generation Sequencing-Based Diversity Studies. *Nucleic Acids Res.* **2013**, *41*, e1. [CrossRef]
34. Megyes, M.; Borsodi, A.K.; Árendás, T.; Márialigeti, K. Variations in the Diversity of Soil Bacterial and Archaeal Communities in Response to Different Long-Term Fertilization Regimes in Maize Fields. *Appl. Soil Ecol.* **2021**, *168*, 104120. [CrossRef]
35. R Core Team. *R: A Language and Environment for Statistical Computing*; R Foundation for Statistical Computing: Vienna, Austria, 2023. Available online: https://www.r-project.org/ (accessed on 31 January 2026).
36. Callahan, B.J.; McMurdie, P.J.; Rosen, M.J.; Han, A.W.; Johnson, A.J.A.; Holmes, S.P. DADA2: High-Resolution Sample Inference from Illumina Amplicon Data. *Nat. Methods* **2016**, *13*, 581–583. [CrossRef]

37. Quast, C.; Pruesse, E.; Yilmaz, P.; Gerken, J.; Schweer, T.; Yarza, P.; Peplies, J.; Glöckner, F.O. The SILVA Ribosomal RNA Gene Database Project: Improved Data Processing and Web-Based Tools. *Nucleic Acids Res.* **2013**, *41*, 590–596. [CrossRef]
38. McMurdie, P.J.; Holmes, S. Phyloseq: An R Package for Reproducible Interactive Analysis and Graphics of Microbiome Census Data. *PLoS ONE* **2013**, *8*, e61217. [CrossRef]
39. Graves, S.; Piepho, H.; Selzer, L.; Dorai-Raj, S. multcompView: Visualizations of Paired Comparisons. R Package Version 0.1.10. Available online: https://CRAN.R-project.org/package=multcompView (accessed on 3 November 2025).
40. Wickham, H. *ggplot2: Elegant Graphics for Data Analysis*, R Package Version: 4.0.1; Springer: New York, NY, USA, 2016. Available online: https://ggplot2.tidyverse.org (accessed on 31 January 2026).
41. Kolde, R. pheatmap: Pretty Heatmaps; R Package Version 1.0.13. 2025. Available online: https://CRAN.R-project.org/package=pheatmap (accessed on 3 November 2025).
42. Wickham, H.; François, R.; Henry, L.; Müller, K.; Vaughan, D. dplyr: A Grammar of Data Manipulation, Package Version 1.1.4. 2023. Available online: https://CRAN.R-project.org/package=dplyr (accessed on 3 November 2025).
43. Oksanen, J.; Blanchet, F.G.; Friendly, M.; Kindt, R.; Legendre, P.; McGlinn, D.; Minchin, P.R.; O'Hara, R.B.; Simpson, G.L.; Solymos, P.; et al. vegan: Community Ecology Pack. R Package Version 2.6.10. 2025. Available online: https://CRAN.R-project.org/package=vegan (accessed on 3 November 2025).
44. Mallick, H.; Rahnavard, A.; McIver, L.J.; Ma, S.; Zhang, Y.; Nguyen, L.H.; Tickle, T.L.; Weingart, G.; Ren, B.; Schwager, E.H.; et al. Multivariable Association Discovery in Population-Scale Meta-Omics Studies. *PLoS Comput. Biol.* **2021**, *17*, e1009442. [CrossRef]
45. Sannino, C.; Qi, W.; Rüthi, J.; Stierli, B.; Frey, B. Distinct Taxonomic and Functional Profiles of High Arctic and Alpine Permafrost-Affected Soil Microbiomes. *Environ. Microbiome* **2023**, *18*, 54. [CrossRef]
46. Waldrop, M.P.; Chabot, C.L.; Liebner, S.; Holm, S.; Snyder, M.W.; Dillon, M.; Dudgeon, S.R.; Douglas, T.A.; Leewis, M.C.; Walter Anthony, K.M.; et al. Permafrost Microbial Communities and Functional Genes Are Structured by Latitudinal and Soil Geochemical Gradients. *ISME J.* **2023**, *17*, 1224–1235. [CrossRef]
47. Varsadiya, M.; Urich, T.; Hugelius, G.; Barta, J. Microbiome Structure and Functional Potential in Permafrost Soils of the Western Canadian Arctic. *FEMS Microbiol. Ecol.* **2021**, *97*, 8. [CrossRef]
48. Ali, A.; Vishnivetskaya, T.A.; Chauhan, A. Comparative Analysis of Prokaryotic Microbiomes in High-Altitude Active Layer Soils: Insights from Ladakh and Global Analogues Using In-Silico Approaches. *Braz. J. Microbiol.* **2024**, *55*, 2437–2452. [CrossRef] [PubMed]
49. Gantner, S.; Andersson, A.F.; Alonso-Sáez, L.; Bertilsson, S. Novel Primers for 16S RRNA-Based Archaeal Community Analyses in Environmental Samples. *J. Microbiol. Methods* **2011**, *84*, 12–18. [CrossRef]
50. Kang, L.; Song, Y.; Mackelprang, R.; Zhang, D.; Qin, S.; Chen, L.; Wu, L.; Peng, Y.; Yang, Y. Metagenomic Insights into Microbial Community Structure and Metabolism in Alpine Permafrost on the Tibetan Plateau. *Nat. Commun.* **2024**, *15*, 5920. [CrossRef] [PubMed]
51. Waqas, M.; Liebmann, P.; Vogel, C.; Varsadiya, M.; Wang, H.; Shibistova, O.; Novák, M.; Urich, T.; Guggenberger, G.; Bárta, J. Different Hydrological Conditions after Permafrost Thaw Result in Distinct Microbial Community Compositions. *bioRxiv* **2024**. [CrossRef]
52. Wu, X.; Xu, H.; Liu, G.; Ma, X.; Mu, C.; Zhao, L. Bacterial Communities in the Upper Soil Layers in the Permafrost Regions on the Qinghai-Tibetan Plateau. *Appl. Soil Ecol.* **2017**, *120*, 81–88. [CrossRef]
53. Neilson, J.W.; Quade, J.; Ortiz, M.; Nelson, W.M.; Legatzki, A.; Tian, F.; LaComb, M.; Betancourt, J.L.; Wing, R.A.; Soderlund, C.A.; et al. Life at the Hyperarid Margin: Novel Bacterial Diversity in Arid Soils of the Atacama Desert, Chile. *Extremophiles* **2012**, *16*, 553–566. [CrossRef]
54. Bull, A.T.; Idris, H.; Sanderson, R.; Asenjo, J.; Andrews, B.; Goodfellow, M. High Altitude, Hyper-Arid Soils of the Central-Andes Harbor Mega-Diverse Communities of Actinobacteria. *Extremophiles* **2018**, *22*, 47–57. [CrossRef]
55. Medina Caro, D.; Bartholomäus, A.; García, A.; Oses, R.; Liebner, S.; Wagner, D. Metabolic Transitions along a Moisture Gradient in a Poly-Extreme High-Altitude Desert Ecosystem within the Atacama Desert. *Environ. Microbiome* **2026**, *21*, 20. [CrossRef]
56. Mohammadipanah, F.; Wink, J. Actinobacteria from Arid and Desert Habitats: Diversity and Biological Activity. *Front. Microbiol.* **2016**, *6*, 1541. [CrossRef]
57. Filippidou, S.; Junier, T.; Wunderlin, T.; Kooli, W.M.; Palmieri, I.; Al-Dourobi, A.; Molina, V.; Lienhard, R.; Spangenberg, J.E.; Johnson, S.L.; et al. Adaptive Strategies in a Poly-Extreme Environment: Differentiation of Vegetative Cells in Serratia Ureilytica and Resistance to Extreme Conditions. *Front. Microbiol.* **2019**, *10*, 102. [CrossRef]
58. Dieser, M.; Battista, J.R.; Christner, B.C. DNA Double-Strand Break Repair at −15 °C. *Appl. Environ. Microbiol.* **2013**, *79*, 7662. [CrossRef] [PubMed]
59. Ma, Y.; Wang, J.; Liu, Y.; Wang, X.; Zhang, B.; Zhang, W.; Chen, T.; Liu, G.; Xue, L.; Cui, X. Nocardioides: "Specialists" for Hard-to-Degrade Pollutants in the Environment. *Molecules* **2023**, *28*, 7433. [CrossRef]
60. Jiang, Z.M.; Mou, T.; Sun, Y.; Su, J.; Yu, L.Y.; Zhang, Y.Q. Environmental Distribution and Genomic Characteristics of Solirubrobacter, with Proposal of Two Novel Species. *Front. Microbiol.* **2023**, *14*, 1267771. [CrossRef] [PubMed]

61. Orellana, R.; Macaya, C.; Bravo, G.; Dorochesi, F.; Cumsille, A.; Valencia, R.; Rojas, C.; Seeger, M. Living at the Frontiers of Life: Extremophiles in Chile and Their Potential for Bioremediation. *Front. Microbiol.* **2018**, *9*, 2309. [CrossRef] [PubMed]
62. Vishnivetskaya, T.A.; Almatari, A.L.; Spirina, E.V.; Wu, X.; Williams, D.E.; Pfiffner, S.M.; Rivkina, E.M. Insights into Community of Photosynthetic Microorganisms from Permafrost. *FEMS Microbiol. Ecol.* **2020**, *96*, 229. [CrossRef] [PubMed]
63. Rego, A.; Raio, F.; Martins, T.P.; Ribeiro, H.; Sousa, A.G.G.; Séneca, J.; Baptista, M.S.; Lee, C.K.; Craig Cary, S.; Ramos, V.; et al. Actinobacteria and Cyanobacteria Diversity in Terrestrial Antarctic Microenvironments Evaluated by Culture-Dependent and Independent Methods. *Front. Microbiol.* **2019**, *10*, 1018. [CrossRef] [PubMed]
64. Bartholomäus, A.; Genderjahn, S.; Mangelsdorf, K.; Schneider, B.; Zamorano, P.; Kounaves, S.P.; Schulze-Makuch, D.; Wagner, D. Inside the Atacama Desert: Uncovering the Living Microbiome of an Extreme Environment. *Appl. Environ. Microbiol.* **2024**, *90*, e0144324. [CrossRef] [PubMed]
65. Wright, C.L.; Lehtovirta-Morley, L.E. Nitrification and beyond: Metabolic Versatility of Ammonia Oxidising Archaea. *ISME J.* **2023**, *17*, 1358–1368. [CrossRef]
66. Verhamme, D.T.; Prosser, J.I.; Nicol, G.W. Ammonia Concentration Determines Differential Growth of Ammonia-Oxidising Archaea and Bacteria in Soil Microcosms. *ISME J.* **2011**, *5*, 1067. [CrossRef]

Disclaimer/Publisher's Note: The statements, opinions and data contained in all publications are solely those of the individual author(s) and contributor(s) and not of MDPI and/or the editor(s). MDPI and/or the editor(s) disclaim responsibility for any injury to people or property resulting from any ideas, methods, instructions or products referred to in the content.